Evaluation of Kinetic Parameters for Two-step Analysis in Nodal Code KANT

Taesuk Oh [a], Yunseok Jeong [a], Junwoo Lee [a] and Yonghee Kim [a*]
[a] *Nuclear and Quantum Engineering, Korea Advanced Institute of Science and Technology (KAIST), 291 Daehak-ro, Yuseong-gu, Daejeon 34141, Republic of Korea*
[*] *Corresponding author: yongheekim@kaist.ac.kr*

***Keywords :** Kinetic Parameters, Two-step Analysis, Nodal Code KANT

1. Introduction

In designing pressurized water reactors (PWR) and conducting safety analyses, it is essential to evaluate the steady-state multiplication factor, burnup-dependent characteristics, and dynamic behavior of the reactor system. For balancing accuracy and computational efficiency, the conventional 'two-step' methodology, which can be found in various code suites including Serpent2/ARES, DeCART/MASTER, SCALE/PARCS, and CASMO/SIMULATE, remains fundamental in modern reactor analysis [1-4]. These systems use transport calculations for assembly-level analysis, i.e., lattice calculation, which is then condensed or homogenized into few-group cross-sections for performing diffusion calculation for whole core analysis.

The accuracy of the final results in whole core calculations using the two-step procedure largely depends on how well the high-fidelity information from the transport-based lattice calculation is preserved. To achieve this, various homogenization techniques, such as the generalized equivalence theory (GET) or super-homogenization (SPH) are commonly employed [5-6]. For deducing pin-power distribution, form-function or embedded pin power reconstruction (EPPR) measures can be taken [7].

All of the aforementioned aspects of the two-step analysis have been extensively studied and are now considered fundamental requirements for modern nodal codes. However, the evaluation of kinetic parameters within the two-step methodology has received relatively less attention. Since the dynamic behavior of a reactor is highly dependent on these parameters, their accurate assessment is equally important. In this work, we present preliminary results from evaluating kinetic parameters using the nodal code KANT [8].

2. Nodal Code KANT

In this section, a brief remark for the nodal code KANT (KAIST Advanced Nodal Tachygraphy) is presented, which is a multi-physics three-dimensional space-time PWR simulator [8]. It solves the neutron diffusion equation in Cartesian geometries based on the Nodal Expansion Method (NEM) accelerated through various coarse-mesh finite difference (CMFD) schemes. Recently, the Source Expansion Nodal Method (SENM) feature has been included [9].

For achieving nodal equivalence, discontinuity factors are applied to every surface of a computational node, including the axial direction in KANT. To account for thermal-hydraulic feedback effects, KANT incorporates a simplified thermal-hydraulics module. For depletion analysis, a so-called predictor-corrector scheme-based macroscopic depletion method is employed, with special attention given to xenon and samarium decay chains.

Figure 1 illustrates the overall flowchart of the two-step analysis procedure using KANT, where both the deterministic transport code DeCART2D and the Monte Carlo-based transport code Serpent2 can serve as the lattice code. Additional details about the KANT nodal code are available elsewhere [8].

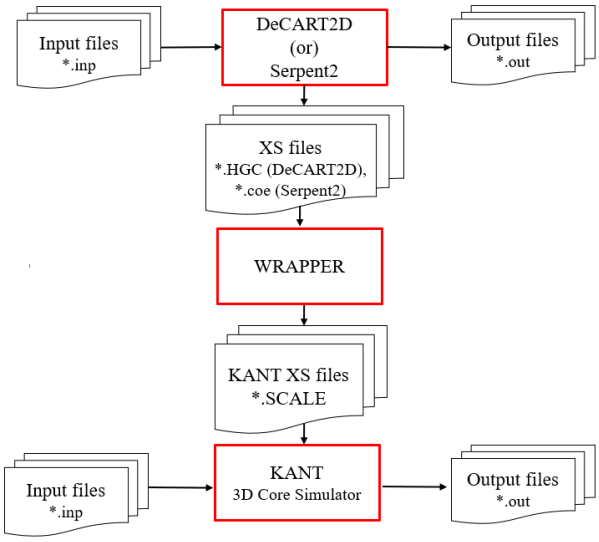

Fig 1. Flowchart of two-step calculation using KANT.

3. Evaluation of Kinetic Parameters

As aforementioned, the lattice calculation result is homogenized to generate few-group cross-sections and discontinuity factors. Alongside, the effective kinetic parameters, i.e., adjoint flux-weighted kinetic parameters, can be generated. For instance, the effective delayed neutron fraction for the k^{th} group ($\beta_{d,k}$) is obtained as:

$$\beta_{d,k} = \frac{\left\langle \varphi^{\dagger}(\vec{r},E,\vec{\Omega}), \frac{\chi_{d,k}(E)}{4\pi} F_{d,k}\varphi(\vec{r},E,\vec{\Omega}) \right\rangle}{\left\langle \varphi^{\dagger}(\vec{r},E,\vec{\Omega}), \frac{\chi(E)}{4\pi} F\varphi(\vec{r},E,\vec{\Omega}) \right\rangle}, \quad (1)$$

where bracket denotes phase-space integration, $\varphi^{\dagger}$ is the adjoint flux, and all the other notations are that of the convention. Similarly, the effective decay constant for each precursor group and energy-dependent neutron speed can be assessed, which is necessary information for performing transient analysis.

The adjoint flux information in Eq. (1) can be directly calculated when deterministic transport approach is used. For Monte Carlo (MC) simulations, the Iterated Fission Probability (IFP) method is often employed to assess adjoint flux-weighted parameters. Comprehensively, the procurement of assembly-wise effective kinetic parameters during lattice calculation can be readily achieved analogous to that of few-group cross-sections.

3.1 Effective Kinetic Parameters for Whole Core

While assembly-wise effective kinetic parameters can be obtained and tabulated during the lattice calculation, additional analysis is required to determine the kinetic parameters for the entire reactor core. This analysis must account for the core configuration, including the fuel loading scheme and burnup distribution. As burnup progresses, U-238 is converted into Pu-239, leading to a significant reduction in the delayed neutron fraction. Although a batch-wise fuel shuffling scheme would mitigate the differences in this value between the beginning of cycle (BOC) and end of cycle (EOC), the deviation remains non-negligible.

Additionally, the adjoint flux information obtained in Eq. (1) during the lattice calculation may differ from that in the whole core scenario. Currently, there is no established method to quantify nor bridge the disparity between the adjoint flux from lattice calculations and that from the whole core analysis. However, based on our best estimation, the effective kinetic parameters in the KANT nodal code are evaluated as follows:

$$\beta_{d,k,core} = \frac{\sum_{i=1}^{N}\sum_{g=1}^{G} \varphi_{i,g}^{\dagger} \beta_{d,k,i} \varphi_{i,g}}{\sum_{i=1}^{N}\sum_{g=1}^{G} \varphi_{i,g}^{\dagger} \varphi_{i,g}}, \qquad (2)$$

where subscripts i and g denote node and group index during the nodal calculation. Note that similar approach can be taken for calculating precursor decay constant and neutron speed concerning the whole core.

From the forward calculation, the flux distribution can be obtained. However, to calculate Eq. (2), the adjoint flux distribution from the whole core analysis is required. Details regarding the process of obtaining the adjoint flux distribution in KANT will be discussed in the following section.

3.2 Assessment of Adjoint Flux Distribution

The evaluation of adjoint flux can be carried out by either solving the balance equation directly for the adjoint flux or by solving the transposed balance equation for the forward flux. These approaches are commonly known as the physical adjoint flux method and the mathematical adjoint flux method, respectively.

The concept of physical adjoint flux, derived by discretizing the balance equation specifically for adjoint flux, remains somewhat ambiguous. The inclusion of discontinuity factors or super-homogenization factors further complicates its interpretation.

In contrast, the mathematical adjoint, obtained by solving the transposed balance equation for the forward flux, is more straightforward. However, directly transposing the continuous balance equation, especially when forward flux is computed using nodal methods involving transverse leakage, is neither practical nor intuitive. An alternative approach involves transposing the discretized balance equation within CMFD-accelerated nodal methods, where transverse leakage and related complexities are addressed through correction factors in the migration matrix (M).

$$M\varphi = \frac{1}{k_{eff}} F\varphi, \qquad (3a)$$

$$M^{T}\varphi^{\dagger} = \frac{1}{k_{eff}} F^{T}\varphi^{\dagger}. \qquad (3b)$$

This method, known as the numerical adjoint, is the one implemented in KANT [10].

4. Numerical Results

In the KANT code, the effective kinetic parameters for the entire core are derived using Eq. (2). This process utilizes the node-wise numerical adjoint flux distribution, which is influenced by the specific acceleration scheme used, as correction factors are incorporated into the migration matrix. The calculation can employ one of the following CMFD schemes: conventional CMFD, partial current-based CMFD (p-CMFD), or one-node CMFD.

In this study, a UOX-loaded 2D SMR core, depicted in Figure 2, has been selected for analysis. Each fuel assembly consists of a 16x16 array of fuel rods with a pitch of 1.2658 cm. Both the whole core depletion calculation and lattice calculation were conducted using Serpent2.2.0 [11]. The calculation conditions are summarized in Table 1.

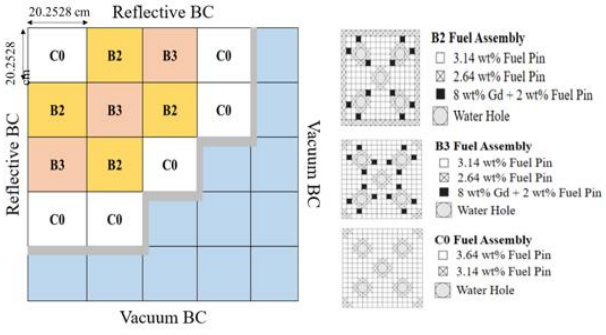

Fig 2. Illustration of the UOX-loaded 2D SMR core.

Table 1. Whole core and lattice calculation conditions.

Type	Histories per cycle	# Inactive Cycles	# Active Cycles
Whole Core	1,000,000	100	200
Lattice	2,000,000	100	500

Two-group homogenized cross-sections have been generated, with reflector region values obtained from the whole core analysis. For the fuel assemblies, the cross-sections and Assembly Discontinuity Factors (ADFs) were determined based on lattice calculations as discussed above.

The KANT nodal code employed both NEM and SENM kernels with subdivision of each assembly into a 2x2 configuration. The multiplication factor and power density distribution for the initial core, i.e., no burnup considered, are presented in Table 2 and Figure 3. These results are compared with the reference Monte Carlo simulation data.

Table 2. Multiplication Factor

CASE	k_{eff}	Δρ [pcm]
Reference	1.07416 ± 4.7	-
NEM (2x2)	1.07373	-37.0
SENM (2x2)	1.07373	-37.5

3.415 -2.05 -2.01	1.586 -1.95 -1.94	0.802 -0.33 -0.31	0.588 4.69 4.60
	1.032 -1.53 -1.50	0.645 2.02 2.00	0.417 5.42 5.30
Reference NEM (%) SENM (%)		0.476 5.27 5.19	

Fig 3. Normalized power density distribution. Relative error with respect to the reference is shown.

The nodal calculation results are independent of the type of CMFD acceleration used. However, the numerical adjoint flux exhibits significant differences, particularly in the p-CMFD case, as shown in Figures 4 and 5, which depict the normalized fast- and thermal-group numerical adjoint flux distributions for the NEM calculation, respectively. A similar pattern is observed for the numerical adjoint flux derived using the SENM kernel (details omitted in the manuscript for brevity)

Such a deviation stems from the fact that p-CMFD correction factors render the group-wise migration to be non-self-adjoint. Consequently, one could expect that the calculated effective kinetic parameters, i.e., Eq. (2), would vary depending on the type of acceleration.

Figure 6 illustrates the evolution of the multiplication factor and reactivity difference over the course of the depletion calculation. Both NEM and SENM kernels were utilized, revealing only marginal differences between them. It is important to note that the evolution

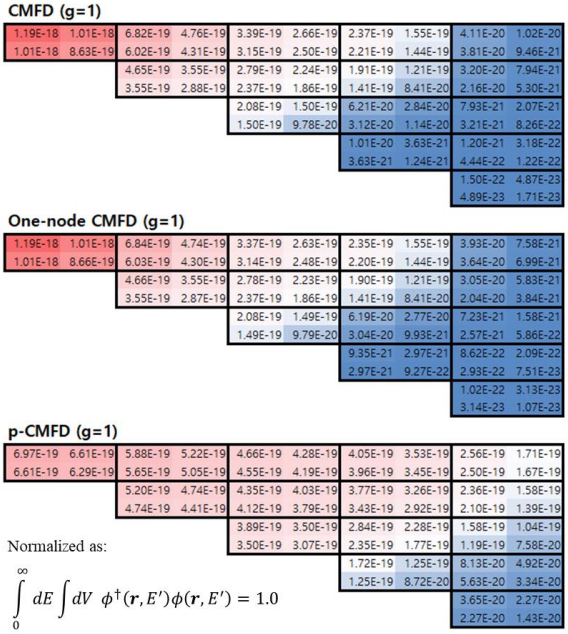

Fig 4. Numerical adjoint flux distribution for NEM (g=1).

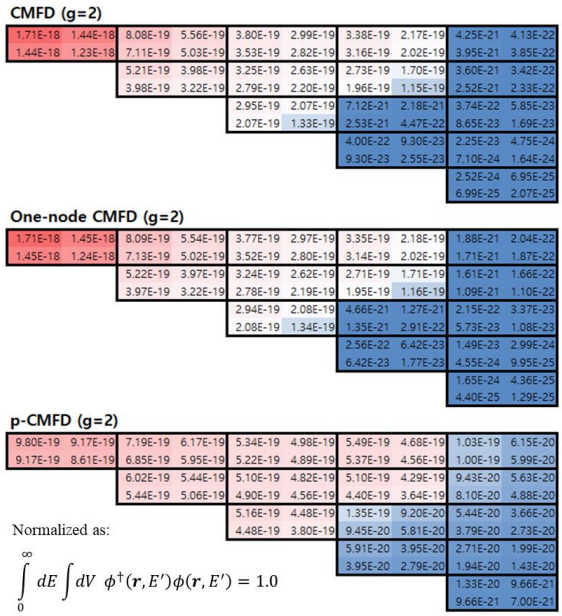

Fig 5. Numerical adjoint flux distribution for NEM (g=2).

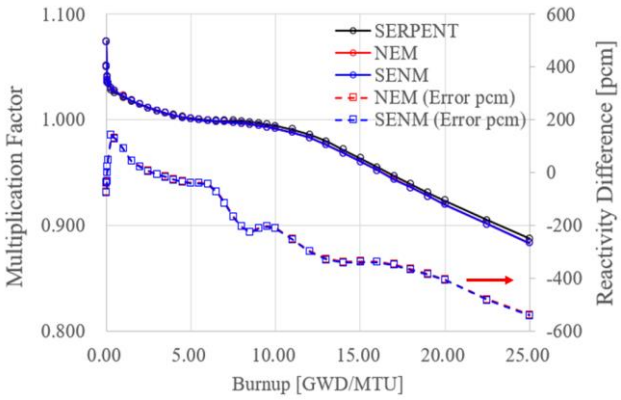

Fig 6. Depletion calculation result.

of the multiplication factor during depletion is independent of the type of acceleration scheme employed. The reference Serpent MC result exhibited an apparent uncertainty of approximately 5 pcm overall.

Figure 7 illustrates the evolution of the core's effective delayed neutron fraction at each burnup step, with results based on the NEM kernel while varying the CMFD types. Additionally, results using a unit vector in place of adjoint flux information are included for comparison (legend: UNITY). The CMFD and one-node CMFD results closely resemble each other, showing the least deviation from the reference. In contrast, the p-CMFD results exhibit less accurate estimations, attributable to differences in the numerical adjoint flux. The unit vector case produces the largest deviation, underscoring the importance of adjoint flux information for accurately estimating nodal-based kinetic parameters.

Given that the adjoint flux distribution is insensitive to the kernel type, similar trends are expected in the estimated kinetic parameters. Figure 8 compares the evolution of the effective delayed neutron fraction for the NEM and SENM kernel cases, where no significant differences are observed. Note that the conventional CMFD acceleration was employed.

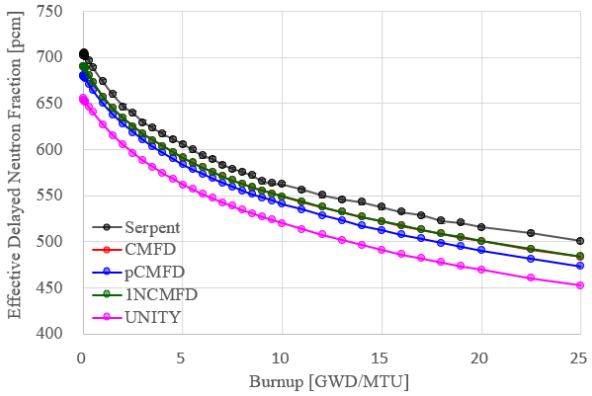

Fig 7. Calculated whole core β_{eff}. (NEM-kernel used)

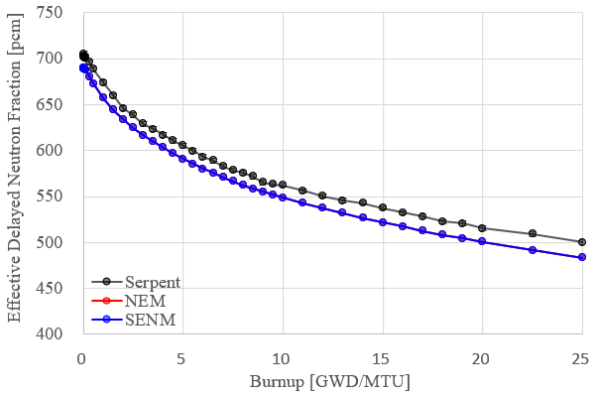

Fig 8. Calculated whole core β_{eff}. (CMFD used)

5. Conclusions

The work presented demonstrates the capability of the nodal code KANT in assessing effective kinetic parameters within the context of two-step analysis. Assembly-wise kinetic parameters are calculated during the lattice calculation and tabulated similarly to few-group homogenized cross-sections. The numerical adjoint flux distribution, obtained by transposing the system matrix, is then used to calculate the whole core kinetic parameters.

It was found that the delayed neutron fraction is dependent on the type of CMFD acceleration used, particularly in the case of p-CMFD. The correction factors in the p-CMFD method cause the migration matrix to become non-self-adjoint, which is unphysical and results in larger deviations in the calculated effective kinetic parameters. It is important to note that other forward calculation-related quantities, such as the multiplication factor and power distribution, are unaffected by the type of acceleration used. Additionally, no significant difference in the delayed neutron fraction was observed when employing different kernels during the nodal calculation. Overall, the findings suggest that using CMFD or one-node CMFD is preferable for evaluating kinetic parameters for the whole core.

AWKNOWLEDGEMENTS

This work was supported by the National Research Foundation of Korea (NRF) Grant funded by the Korean Government (MSIT) (RS-2022-00144429, and 2022M2E9A304619013).

REFERENCES

[1] Jaakko Leppänen, Riku Mattila, (2016). Validation of the Serpent-ARES code sequence using the MIT BEAVRS benchmark – HFP conditions and fuel cycle 1 simulations. Annals of Nuclear Energy 96. 324–331.
[2] Jin Young Cho, et al, (2013). Three-dimensional nuclear analysis system DeCART/CHORUS/MASTER. ANS Annual Meeting, Atlanta, June 16-20.
[3] Piotr Darnowski, Michał Pawluczyk, 2019. Analysis of the BEAVRS PWR benchmark using SCALE and PARCS. NUKLEONIKA 64(3): 87-96.
[4] SSP-09/447-U, (2009). SIMULATE-3: Advanced Three-Dimensional Two-Group Reactor Analysis Code User's Manual, Studsvik Scandpower.
[5] K. S. Smith (1986), "Assembly Homogenization Techniques for Light Water Reactor Analysis", Progress in Nuclear Energy, Vol. 17, No. 3, pp 303-335
[6] A. Hebert (1993), "A Consistent Technique for the Pin-by-Pin Homogenization of a Pressurized Water Reactor Assembly", *Nuclear Science and Engineering*, 113:3, 227-238
[7] H. Yu, S. Jang, Y. Kim, (2021). A New Embedded Analysis with Pinwise Discontinuity Factors for Pin Power Reconstruction. Nuclear Science and Engineering, 195:7.
[8] Taesuk Oh, et al., (2023). Development and validation of multiphysics PWR core simulator KANT, Nuclear Engineering and Technology, vol. 55, no. 6 pp. 2230–2245
[9] Y. I. Kim, Y. J. Kim, S. J. Kim, T. K. Kim, (1999) "A Semi Analytic Multigroup Nodal Method," Ann. Nucl. Eng., Vol. 26, No. 8, pp. 699-708.
[10] Taesuk Oh and Yonghee Kim, (2022), "Investigation of Nodal Numerical Adjoints from CMFD-Based Acceleration Methods," Front. Energy Res. 10:873731.
[11] J. Leppänen, et al., (2015), "The Serpent Monte Carlo code: Status, development and applications in 2013," Ann. Nucl. Energy, vol. 82, pp. 142–150.